Single-crystal neutron diffraction study of the structural phase transition in $Ba_{0.95}Ca_{0.05}TiO_3$

1996 J. Phys.: Condens. Matter 8 2905

(http://iopscience.iop.org/0953-8984/8/16/020)

J. Phys.: Condens. Matter **8** (1996) 2905–2913. Printed in the UK

Single-crystal neutron diffraction study of the structural phase transition in $Ba_{0.95}Ca_{0.05}TiO_3$

P U M Sastry†, A Sequeira†, H Rajagopal†, B A Dasannacharya†, S Balakumar‡, R Ilangovan‡ and P Ramasamy‡

† Solid State Physics Division, Bhabha Atomic Research Centre, Trombay, Bombay 400085, India

‡ Crystal Growth Centre, Anna University, Madras 600025, India

Received 3 October 1995, in final form 12 December 1995

Abstract. The tetragonal-to-cubic transition in ferroelectric $Ba_{0.95}Ca_{0.05}TiO_3$ (BCT) has been studied using a single-crystal neutron diffraction technique. The intensities of the Bragg profiles are observed to increase anomalously with temperature above 110 °C are then to drop sharply before reaching the structural transition temperature T_0. The intensity variations and T_0 are sensitive to sample heating rate with $T_0 = 145$ °C at slow heating rates. Structural refinements indicate that the observed intensity variations are due to changes in the domain structure and the thermal parameters B with the latter becoming anomalously large several degrees Celsius below T_0 compared with those above T_0 and at room temperature, indicating the onset of significant pre-transition disorder for Ti ions along the polar c axis. The observed linewidths of the diffraction profiles reflect contributions from the anisotropic domain sizes and the internal strains and an added contribution from the coexistence of tetragonal and cubic phases below T_0. The results suggest that the fluctuations in the Ti positions existing well below T_0 could be responsible for the broadening of dielectric response observed for BCT.

1. Introduction

The paraelectric-to-ferroelectric transition in $BaTiO_3$ is accompanied by a change in the crystal structure from cubic to tetragonal symmetry. Close to the transition temperature, $BaTiO_3$ crystallites are known [1] to form a large number of small domains (about 100 to 1000 Å in size), the so-called Kanzig regions [2], whose spontaneous polarization is controlled by thermal fluctuations [1]. It is also known that the Curie temperature of $BaTiO_3$ decreases linearly with increase in stress of the sample [3]. Accordingly, the observed broadening of dielectric response together with a range of Curie temperatures of the substituted samples such as $Ba(Ti,Sn)O_3$ [4] and $Ba(Ti,Zr)O_3$ [5] have been attributed [2] to fluctuations in the dopant concentration and the concomitant stress variations. Such transitions are termed diffuse phase transitions (DPTs) [6]. On the other hand, the DPT in single-crystal $(Ba/Sr)TiO_3$ has been attributed [7] to an intrinsic feature of the transition rather than to compositional inhomogeneities. Recently, it has been suggested [8] that disorder in ABO_3-type ferroelectrics, arising from the substitutions either at the A sites or at the B sites can also lead to a DPT. For example, the FCC phase of $Pb(Sc,Ta)O_3$ exhibits a sharp transition with ordered distributions of Sc and Ta at B sites, whereas in the simple cubic phase the transition becomes more and more broadened with increasing disorder at B sites [9].

0953-8984/96/162905+09$19.50

Most of the structural studies of the DPT in doped ABO_3-type compounds are based on polycrystalline samples and could yield only limited information on the transition behaviour. In order to throw further light on the nature of the DPT, we have carried out a single-crystal neutron structural study of $Ba_{0.95}Ca_{0.05}TiO_3$ in the temperature range from 30 to 150 °C.

2. Experiment

Single crystals of BCT were grown by Remeika's technique with the nominal Ca ion concentration of 8 at.%, as described earlier [10]. A composition analysis using optical emission technique, however, indicated [11] a Ca ion concentration of only about 5 at.%. A crystal of size 1.3 mm × 2.0 mm × 3.8 mm (cut from an as-grown crystal) was mounted on an Enraf–Nonius high-temperature goniometer which in turn was mounted on a four-circle neutron diffractometer at the Dhruva reactor with the crystal b axis along the ϕ axis. The crystal was heated by blowing a stream of hot air over it, and the temperature was measured with a chromel–alumel thermocouple placed near the crystal. The temperature stability was maintained to within ±1 °C throughout the experiment. The crystal was heated to 150 °C and cooled to room temperature (RT) repeatedly until the observed Bragg intensities at RT yielded reproducible values after equilibrating the crystal for thermal cycling effects across the transition. The tetragonal-to-cubic (T → C) transition was monitored by recording the diffraction profiles of (002) and (200) reflections at several temperatures. The transition behaviour was observed to depend on the rate of heating. Consequently, the profiles were scanned by heating the crystal at two heating rates: a slow rate of 10 °C h^{-1} and a fast rate of 5 °C min^{-1}. In the slow-heating case, the temperature was raised in steps of 10 °C and the intensities were recorded after the crystal was allowed to remain at each temperature for about an hour during which the Bragg intensities were observed to equilibrate. In the fast-heating process, the crystal temperature was raised in steps of 10 °C per 2 min and at each step the Bragg intensities of (002) and (200) were recorded within an interval of 5 min. For the purpose of structure refinements, diffracted intensities for a set of reflections, in an octant of reciprocal space within the limit $(\sin\theta)/\lambda = 0.5$ Å^{-1} ($\lambda = 1.216$ Å), were recorded in a θ–2θ step scanning mode at RT, 90 °C and 120 °C in the tetragonal phase and at 150 °C in the cubic phase by heating the crystal in the slow-heating mode. The cell parameters and crystal orientation were refined using the optimized 2θ and orientation angles for the strong reflections. The scan lengths included at least ten background steps on either side of the peak. Intensity fluctuations in the standard reflections (002) and (200) were observed to remain within 2% from the mean values during the entire experiment at each temperature, confirming the stability of the crystal. The integrated intensities were reduced to structure factors by applying standard Lorentz and absorption corrections. A calculated absorption coefficient of 0.0114 mm^{-1} was used.

3. Structural refinements

Refinements of the structures at RT, 90 °C, 120 °C and 150 °C were carried out on the basis of the standard perovskite structural model using the full-matrix least squares refinement program TRXFLS [12, 13]. Neutron scattering lengths of 5.25 fm, 4.9 fm, −3.44 fm and 5.8 fm for Ba, Ca, Ti and O atoms, respectively, were used. The quantity minimized was $\sum w(F_o - |F_c|)^2$ and refinements were carried out with the weights w based on counting statistics ($w = \{\sigma_{st}^2(F_o) + (kF_o)^2\}^{-1}$) as well as with unit weights. Refinements based on unit weights yielded somewhat superior fits and were preferred to those based on

the observational weighting scheme. As the data were moderately affected by extinction, an isotropic extinction correction was applied initially using both primary and secondary extinction models [14]. Refinements based on both of these models gave nearly same agreement (R) factors. However, the primary extinction model indicated rather unrealistic domain sizes (about 20 μm at RT) and hence was rejected. As the intensities of equivalent reflections indicated significant anisotropy effects, further refinements were continued using anisotropic secondary extinction corrections. An anisotropic type-II extinction [15] model was preferred as it yielded better fits than the anisotropic type-I model did.

Table 1. Refined parameters obtained using isotropic temperature factors B and anisotropic extinction correction.

		120 °C		
	RT	Ordered	Disordered	150 °C
Space group	$P4mm$	$P4mm$		$Pm3m$
a (Å)	3.982(7)	3.985(2)		3.997(4)
c (Å)	4.025(8)	4.010(2)		3.997
Ba/Ca (0,0,0)				
B (Å^2)	0.59(25)	0.96(30)	0.89(26)	0.56(15)
N	0.93/0.07(2)	0.93/0.07	0.93/0.07	0.93/0.07
Ti[a] (0.5,0.5,$\pm z$)				
z	0.5110(87)	0.507(12)	$\pm$0.547(13)	0.5
B (Å^2)	0.25(26)	1.62(48)	1.16(43)	0.44(19)
O(1) (0.5,0.5,z)				
z	−0.0206(47)	−0.0238(65)	−0.0326(35)	
B (Å^2)	0.56(20)	0.65(31)	0.53(27)	
O(2) (0,0.5,z)				
z	0.4903(62)	0.4975(55)	0.4974(27)	0.5
B (Å^2)	0.76(17)	1.28(26)	1.22(23)	0.64(13)
Extinction parameters[b] (μm^{-2})				
$W_{11}/10^5$	0.109(45)	0.101(75)	0.16(12)	0.0046(11)
$W_{22}/10^5$	0.021(16)	0.28(36)	0.40(51)	0.0014(4)
$W_{33}/10^5$	0.0036(32)	0.017(21)	0.018(27)	0.0007(2)
$R(F)$	0.0223	0.0397	0.0366	0.0177
$wR(F)$	0.0243	0.0412	0.0359	0.0232

[a] In the disordered model, the Ti ions were disordered at (1/2,1/2,z) and (1/2,1/2,$-z$) sites with 50% occupancies at each site.

[b] The extinction parameters W_{ii} are related to the domain sizes as $r_{ii}(\mu\text{m}) = 1/\sqrt{W_{ii}}$.

Initial refinements were carried out using isotropic temperature factors for all phases. Refinement of the occupancy factor indicated that Ca ions are not located at Ti sites but could be at the Ba sites. The refinements of Ca occupancy at all temperatures indicated an average value of 7%. Consequently, the occupancy of Ca ions has been fixed at 7% in all the refinements. Also, refinements assuming 5% Ca occupancy at Ba sites (following composition analysis) did not indicate significant shifts for any of the refined parameters. However, we note that, in view of the limited contrast between the scattering amplitudes of 5.25 fm (for Ba) and 4.9 fm (for Ca), their relative occupancies can only be taken as

indicators. The refined values of isotropic temperature parameters B were observed to be significantly large at 120 °C compared with those at RT and at 150 °C, particularly for the Ti ions. Hence a further set of refinements was attempted, introducing disorder of Ti ions based on the four-site (x, x, z) and eight-site (x, x, x) models proposed in the literature [16] for the tetragonal and cubic phases, respectively, of $BaTiO_3$. These models did not lead to significant improvement in the refinements either at 120 °C or at other temperatures with the observed shifts of the Ti ions from the mean position being much less than their estimated standard deviations (ESDs). However, refinements carried out by disordering Ti ions over two sites ((1/2,1/2,z) and (1/2,1/2,$-z$)) in the tetragonal phase at 120 °C yielded significant improvement in the R-factors with large displacement ($z \approx 0.2$ Å) of Ti ions along the c-axis on either side of the mean position (1/2,1/2,1/2), as indicated in table 1. Refinement involving disorder of the O(2) atoms (which also exhibited a somewhat large B-value at 120 °C) did not indicate any significant oxygen disorder nor lead to any improvements in the R-factors.

Table 2. Parameters obtained on the basis of the refinement using anisotropic temperature parameters B_{ij} and anisotropic extinction correction. The form of the temperature factors used is $\exp[-(1/4)\{(B_{11}/a^2)h^2 + (B_{22}/b^2)k^2 + (B_{33}/c^2)l^2\}]$. N is the occupancy factor.

	RT	120 °C	150 °C
Ba/Ca (0,0,0)			
B_{11}	0.58(20)	0.70(25)	0.58(16)
B_{22}	0.58	0.76	0.62
B_{33}	0.65(27)	0.64(1.6)	0.62
N	0.93/0.07	0.93/0.07	0.93/0.07
Ti (0.5,0.5,z)			
z	0.5136(64)	0.470(41)	0.5
B_{11}	0.16(25)	1.27(51)	0.50(20)
B_{22}	0.16	1.27	0.48
B_{33}	0.26(42)	5.1(15)	0.48
O(1) (0.5,0.5,z)			
z	−0.0212(37)	−0.039(4)	
B_{11}	0.58(18)	0.51(25)	
B_{22}	0.58	0.51	
B_{33}	0.41(29)	2.06(3.35)	
O(2) (0,0.5,z)			
z	0.4876(32)	0.495(5)	0.5
B_{11}	0.79(20)	0.82(25)	0.60(14)
B_{22}	0.77(19)	1.59(25)	0.64(13)
B_{33}	0.54(20)	0.51(77)	0.64
Extinction parameters (μm^{-2})			
$W_{11}/10^5$	0.120(38)	0.21(13)	0.0046(11)
$W_{22}/10^5$	0.029(17)	0.47(61)	0.0014(4)
$W_{33}/10^5$	0.0045(35)	0.017(27)	0.0007(2)
$R(F)$	0.0218	0.0291	0.0174
$wR(F)$	0.0237	0.0295	0.0229

The structural parameters obtained with isotropic temperature factors were refined further by using anisotropic temperature factors which led to a significant improvement

in the R-values at 120 °C but not at RT and 150 °C. Nevertheless the final R-values at 120 °C are somewhat higher than at other temperatures essentially due to the presence of structural disorder, which cannot be fully accounted for by the anisotropic thermal parameter values, particularly for atoms other than Ti. The disordered Ti-ion model with anisotropic temperature factors yielded fits comparable with those obtained in the model without disorder. While refining the RT and 120 °C data, high correlations between the position parameters, anisotropic temperature factors and extinction parameters were observed. The problem of high correlations among the parameters in the tetragonal phase of pure $BaTiO_3$ at RT has been discussed at length by Harada *et al* [17]. Hence, in the anisotropic temperature factor models, these parameters were varied alternately. The final parameters deduced from isotropic and anisotropic temperature factor models are listed in tables 1 and 2, respectively.

4. Results and discussion

4.1. Peak profiles

The temperature variation in the (002) and (200) peak positions shown in figure 1 indicates a T → C transition temperature T_0 of 145 °C with slow heating rate and 120 °C with fast heating rate. As mentioned in the literature [18] the transition in pure $BaTiO_3$ proceeds by the nucleation-and-growth process, leading to a measured transition temperature which depends on the rate of heating. Thus the observed heating rate dependence of T_0 in BCT is probably due to variations in the nucleation-and-growth rates of the cubic phase with heating rates. The transformation exhibits hysteresis with the reverse transition temperature T_0 (cooling) being about 10 °C lower than T_0 (heating) at both heating rates.

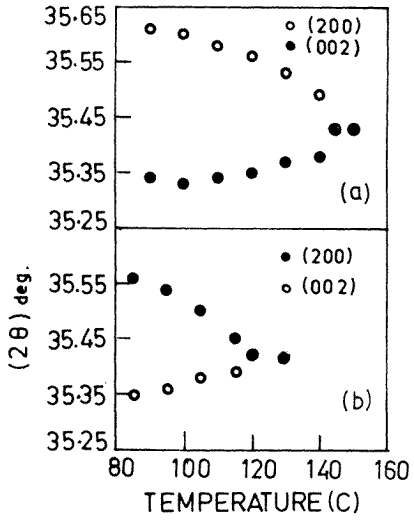

Figure 1. Temperature dependences of profile peak positions at crystal heating rates of (*a*) 10 °C h^{-1} and (*b*) 5 °C min^{-1}.

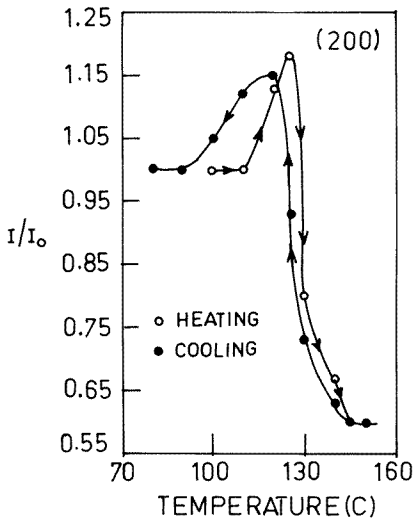

Figure 2. Temperature variation in integrated neutron intensities for (200) reflection at a heating rate of 10 °C h^{-1}: ——, guides to the eye.

The integrated intensities of Bragg profiles exhibit anomalous temperature variations as shown, for example, in figure 2 for (200) reflection. With slow heating rates, the intensity remains almost unchanged from RT to about 110 °C, starts to increase, reaches a maximum

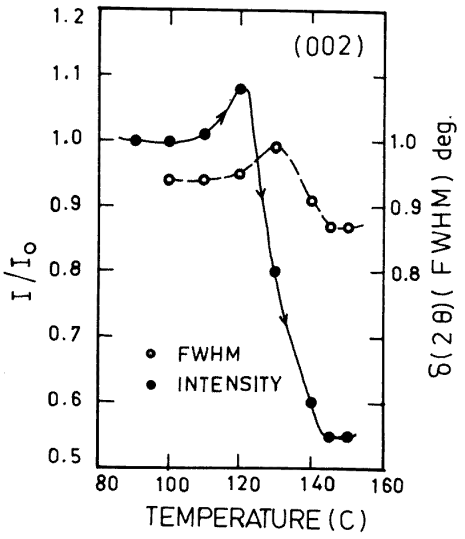

Figure 3. Temperature variations in FWHM and Bragg intensity for (002) reflection: ——, - - - -, guides to the eye.

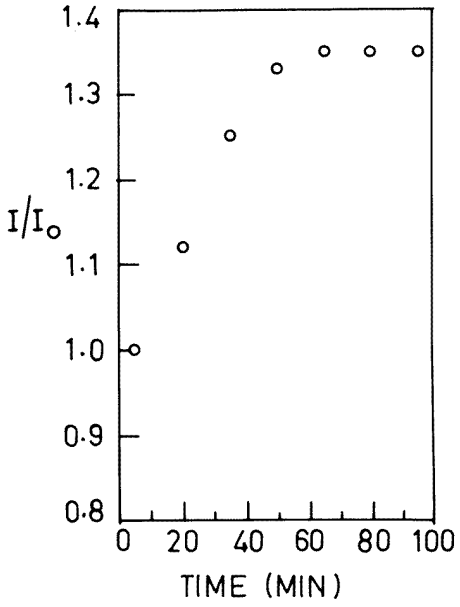

Figure 4. Time variation in Bragg intensity for the (200) reflection after raising the temperature from 110 to 120 °C.

at about 120 °C and then falls between 120 °C and T_0. Figure 3 shows the temperature variation in the full width at half-maximum for (002) with a maximum at 130 °C, which is about 10 °C higher than the temperature of the intensity maximum. The increase in intensities between 110 and 120 °C is associated with a reduction in domain size with increasing temperature (discussed later) in the tetragonal phase, and the subsequent fall in intensities above 120 °C is due to the nucleation and growth of large cubic domains coexisting with tetragonal domains. This is reflected in the broadening of Bragg profiles beyond 120 °C and indicates that the transition in BCT is of the nucleation-and-growth type.

The time variation in the Bragg intensities for BCT attains equilibrium in a short period and reaches a saturation value within about 60 min as indicated in figure 4. In contrast, for (K/Li)TaO_3 (KLT) [19], which shows a glassy transition, the Bragg peaks take days to saturate. This gives further support to the idea that the nature of the transition is of the nucleation-and-growth type. The temperature variation in Bragg intensity for BCT is also different from that observed for KLT. As for KLT, the Bragg intensity for BCT starts to increase on cooling below T_0 but, unlike the situation in the former, the intensity for BCT reaches a maximum and drops again from the maximum on further cooling. It is noteworthy that, in spite of the broad dielectric response of BCT, the nature of the structural transition remains first order as observed in an earlier neutron diffraction study on polycrystalline (Ba/Ca)TiO_3 [20].

4.2. Domain sizes

The refined extinction parameters (table 2) indicate highly anisotropic (ellipsoidal) domains whose size and anisotropy are rather sensitive to temperature. The temperature variation in average domain radius, as deduced from secondary extinction parameters [21] is shown

in figure 5. Average domain sizes ranging from 100 to 1000 Å have been reported [1] near T_0 for pure $BaTiO_3$. Our study shows that the domain sizes in BCT are anisotropic, with the minimum and maximum radial dimensions ranging from 90 to 470 Å at RT, from 45 to 240 Å at 120 °C and from 465 to 1200 Å at 150 °C. The anisotropic nature of the domain sizes is also reflected in the anisotropic broadening of Bragg profiles as shown, for example at RT in figure 6. The average domain radius of about 280 Å at RT obtained from figure 6 using the linewidth analysis [8] is in agreement with the corresponding value (295 Å) estimated from the refined anisotropic secondary extinction parameters (table 2). Together with domain sizes, the domain anisotropy also changes with temperature with the minor axes of the domains being oriented along the *a* axis at RT, along the *b* axis at 120 °C and again along the *a* axis at 150 °C, while the major axes remain along the *c* axis at all temperatures. However, the changes in the domain anisotropy may not be significant when examined by taking into account their ESDs. In order to compare the domain sizes and the orientations at various temperatures, the *a*, *b* and *c* axes of the cubic phase at 150 °C are taken to correspond to the *a*, *b* and *c* axes of the tetragonal cell.

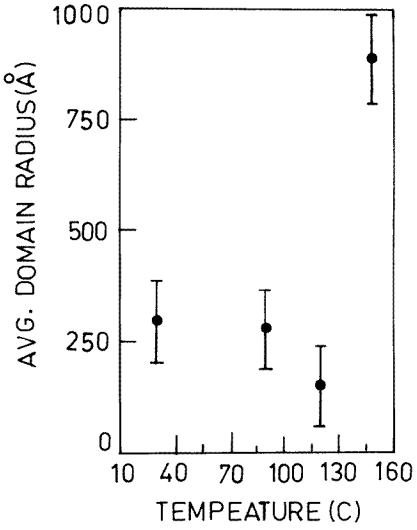

Figure 5. Variation in average domain radius with temperature at a heating rate of 10 °C h^{-1}.

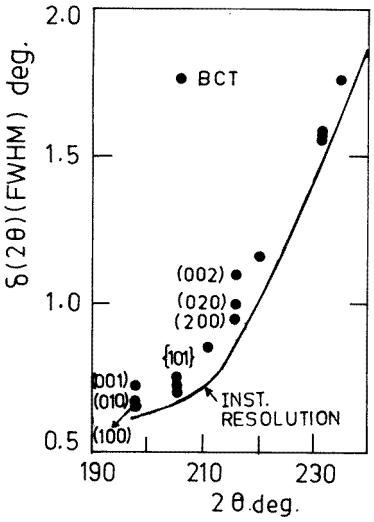

Figure 6. FWHM of Bragg profiles of BCT at RT, indicating the anisotropic linewidths due to anisotropic domain sizes.

4.3. Structural disorder

The refined structural parameters listed in table 1 indicate particularly large *B*-values for Ti ions at 120 °C compared with those at RT and at 150 °C. As indicated in the disorder model, the mean position of the Ti ion at 120 °C is close to (1/2,1/2,1/2) about which it appears to be disordered along the polar *c* axis. The refined anisotropic thermal parameters (table 2) also indicate anomalously large displacements for Ti ions along the *c* axis which is consistent with the result of the disordered isotropic model.

The T → C transition in pure $BaTiO_3$ is believed to have both displacive and order–disorder character. In the displacive (soft-mode) model, the Ti ion in the tetragonal phase is displaced along the ⟨001⟩ direction, which is driven by an unstable optic soft mode whereas,

on the basis of the results of diffuse x-ray scattering, it is proposed [16] that the Ti ions (in both tetragonal and cubic phases) occupy various sites displaced along the permitted ⟨111⟩ directions. Both soft-mode and eight-site models have been extensively discussed in the literature [22–27]. Recent Monte Carlo simulations [26] on $BaTiO_3$ suggested that the transition is intermediate between the displacive and order–disorder limits and indicated a large increase in the displacement vector (from about 0.02 Å above T_0 to about 0.16 Å below T_0) associated with the soft mode.

Our refinements in BCT show insignificant displacements (less than 0.02 Å) for Ti ions in the *a*–*b* plane both at RT (tetragonal) and at 150 °C (cubic) but indicate the presence of Ti disorder involving large displacements along the polar *c* axis at a temperature of 120 °C in the tetragonal phase well below T_0. This is reflected in the anomalously large B_{33}-value (5.1 Å^2, with corresponding $u_{rms} = 0.25$ Å) for the Ti ions at 120 °C. The refined parameters when seen in conjunction with the intensity variations (figure 2) indicate that the onset of Ti disorder along the *c* axis, accompanied by a reduction in the tetragonal (polar) domain sizes, starts to set in at around 110 °C and leads to the observed increase in Bragg intensities above 110 °C. The Ti disorder with large displacements on either side of the central position along the *c* axis averages the dipole moment and may be responsible for the broad dielectric response observed in BCT. Our observation finds further support from the results of recent Raman scattering experiments from our laboratory [28]. The Ti disorder and concomitant reduction in the size of coherent domains in BCT could also be responsible for an enhanced transition temperature T_0.

5. Conclusions

Using the single-crystal neutron diffraction technique we find that, for BCT, there is a gradual reduction in domain sizes with increasing temperature in the tetragonal phase followed by the nucleation and growth of cubic domains during the T → C structural phase transition. The small and highly anisotropic domain sizes and the internal strains contribute to the widths of diffraction profiles. Close to and below the transition temperature T_0, the tetragonal and the cubic phases coexist, reflecting an additional contribution to the width of diffraction profiles. The intensity variations and T_0 depend on the rate of heating of the crystal. Large temperature factors observed at 120 °C indicate significant positional disorder for Ti ions with large displacements about the mean position along the *c* axis well below the transition to the cubic phase. This could be responsible for the broadening of the observed dielectric response observed for BCT. In spite of the broad dielectric response, the transition is observed to be of first order. The nature of the T → C phase transition is different from that for pure $BaTiO_3$ to the extent that the eight-site model does not seem to be applicable for BCT.

Acknowledgments

The authors are grateful to Dr D Pandey who initiated their interest in the problem of the DPT in BCT and with whom they had several discussions. The crystal of BCT was grown by Balakumar, Ilangovan and Ramasamy in Anna University under a BRNS project of the Board of Research in Nuclear Sciences of the Department of Atomic Energy. Authors from the Bhabha Atomic Research Centre have also benefited greatly from discussions with their colleagues Dr A P Roy and Dr M D Sastry.

References

[1] Kanzig W 1951 *Helv. Phys. Acta* **24** 175
[2] Isupov V A 1956 *Sov. Phys.–Tech. Phys.* **1** 1846
[3] Zhaung Z Q, Harmer M P, Smnyth D M and Newnham R E 1987 *Mater. Res. Bull.* **22** 1329
[4] Smolenskii G A and Isupov V A 1954 *J. Tech. Phys. (USSR)* **24** 1375
[5] Smolenskii G A, Tarutin N P and Grudtsin N P 1954 *J. Tech. Phys. (USSR)* **24** 1585
[6] Husson E and Morell A 1992 *Diffusionless Phase Transitions and Related Structures in Oxides* ed C Bullouistix (Aedersmannsdorf: Trans Tech) p 217
Pandey D 1995 *Diffusionless Phase Transitions in Oxides and Some Reconstructive and Martensitic Phase Transitions* ed C Bullouistix (Aedersmannsdorf: Trans Tech) at press
[7] Benguigui L and Bethe K 1976 *J. Appl. Phys.* **47** 2787
[8] Tiwari V S, Pandey D and Groves P 1989 *J. Phys. D: Appl. Phys.* **22** 837
[9] Setter N and Cross L E 1980 *J. Appl. Phys.* **51** 4357
[10] Rajagopal H, Sastry P U M, Sequeira A and Ramasamy P 1994 *Bull. Mater. Sci.* **17** 201
[11] Rao Rekha, Roy A P, Dasannacharya B A, Balakumar S, Ilangovan R, Ramasamy P and Agarwal M D 1995 to be published
[12] Rajogopal H and Sequeira A 1977 A modified version of the program ORFLS [13], unpublished
[13] Busing W R, Martin K O and Levy H A 1962 *Oak Ridge National Laboratory, Oak Ridge, TN, Report* ORNL-TM-305, TM-229
[14] Zachariasen W H 1967 *Acta Crystallogr.* **23** 558
[15] Becker P J and Coppens P 1975 *Acta Crystallogr.* A **31** 417
[16] Comes R, Lambert M and Guinier A 1968 *Solid State Commun.* **6** 715
[17] Hararda J, Pedersen T and Barnea Z 1970 *Acta Crystallogr.* A **26** 336
[18] Darlington C N W, David W I F and Knight K S 1994 *Phase Trans.* **48** 217
[19] Kamitakahara W A, Loong C K, Ostrowski G E and Boatner L A 1987 *Phys. Rev.* B **35** 223
[20] Tiwari V S, Pandey D, Krishna P S R, Chakravarthy R and Dasannacharya B A 1991 *Physica* B **174** 112
[21] Coppens P and Hamilton W C 1970 *Acta Crystallogr.* A **26** 71
[22] Cochran W 1961 *Adv. Phys.* **10** 401
[23] Huller A 1969 *Solid State Commun.* **7** 589
[24] Harada J, Axe J D and Shirane G 1971 *Phys. Rev.* B **4** 155
[25] Dougherty T P, Weiderrecht G P, Nelson K A, Garret M H, Jensen H P and Warde C 1992 *Science* **258** 770
[26] Zhong W, Vanderbilt D and Rabe K M 1994 *Phys. Rev. Lett.* **73** 1861
[27] Sokoloff J P, Chase L L and Rytz D 1988 *Phys. Rev.* B **38** 597
[28] Roy A P, Rekha M A, Dasannacharya B A and Balakumar S 1994 *Int. Conf. on Raman Scattering (Hong Kong, 1994)*